*Int. J. Electrochem. Sci.*, 8 **(2013)** 9107 - 9124

**International Journal of**
**ELECTROCHEMICAL**
**SCIENCE**
www.electrochemsci.org

# Effect of Ti Incorporation on Structure and Oxidation Activity of Ammonium Salt of 12-Molybdophosphoric Acid Catalysts

*Katabathini Narasimharao*[*]

Chemistry Department, Faculty of Science, King Abdulaziz University, P.O.Box 80203, Jeddah 21533, Saudi Arabia
[*]E-mail: katabathini@yahoo.com

*Received:* 26 May 2013 / *Accepted:* 25 June 2013 / *Published:* 1 July 2013

---

The aim of this work is to prepare three series of stoichiometric Ti incorporated ammonium salt of 12-molybdophosphoric acid catalysts in order to study the effect of Ti atoms incorporation on physico-chemical properties of the Keggin structure. Catalysts were prepared by increasing the amounts of Ti atoms from 1 to 3 and a consequence decrease of Mo atoms from 11 to 9 to maintain the stoichiometry of the Keggin unit. Prepared catalysts each subjected to calcination at different temperature in the range 300-500°C. The catalysts were characterized by elemental analysis, powder X-ray diffraction, FTIR, TG, $N_2$ gas adsorption and $^{31}P$ MAS NMR techniques. The redox properties of the Ti incorporated AMPA samples were determined by performing the vapor phase oxidation of benzyl alcohol. Increase of thermal stability, acidity and redox properties with increase of Ti atoms was observed. $AMPTi_3$ catalyst offered highest activity and time on stream analysis revealed that this catalyst is stable under reaction conditions without any deactivation.

---

**Keywords:** Ammonium salt of 12-molybdophosphoric acid, Ti incorporation, oxidation of benzyl alcohol

## 1. INTRODUCTION

Fundamental understanding and determination of reduction potentials (oxidizing capabilities) of heteropolyacid (HPA) catalysts is of great interest in synthesis of HPA catalysts for selective oxidation reactions. Several theoretical (quantum chemical and molecular orbital studies) and instrumental (negative differential resistance and scanning tunneling microscopy) methods have been employed to determine the reduction potentials of HPAs [1, 2]. Conventional electrochemical measurement in solution is the frequently used technique to determine the reduction potentials of HPA catalysts [3]. It is known that the reduction potentials determination via this method is strongly depend on the experimental conditions such as composition of electrolyte solution (pH) and identity of electrodes [4]. Sadakane et al. revealed that [5] direct comparison of reduction potentials of HPA catalysts from literature data is a complex task.

Park et al. [6] observed that the lower absorption edge energy values determined from UV-visible absorption measurements corresponded to the higher reduction potential of the HPA catalysts. These values correlate to redox property (reduction potential and absorption edge energy) of HPA catalysts and catalytic oxidation of benzyl alcohol (formation of benzaldehyde) of the HPA catalysts. The authors also observed that the catalytic oxidation activity increased monotonically with increasing reduction potential and with decreasing absorption edge energy of the HPA catalysts, regardless of the HPA structural difference. Thus, oxidation catalysis of the HPA catalysts can be correlating parameter for the reduction potentials of the HPA catalysts.

Moreover, oxidation of alcohols to aldehydes, in particular benzyl alcohol to benzaldehyde, is an important organic reaction. Benzaldehyde is a very valuable chemical which has widespread applications in perfumery, dyestuff and agro chemical industries [7]. Selective oxidation of alcohols has been extensively studied using various kinds of stiochiometric oxidants such as manganese and chromium salts. However, utilization of these oxidants was restricted due to their toxicity. From the standpoint of atom economy and environmental demand much attention has been paid to the development of metal based catalysts, using clean oxidants, in liquid phase [8].

Athilakshmi and Viswanathan [9] carried out the vapor phase oxidation over MPA and its salts. With the ammonium salt of MPA (AMPA) the reported conversion was about 65% and the benzaldehyde to toluene ratio of 18.9. HPA compounds in protonic form are not stable catalysts in benzyl alcohol atmosphere as they are highly soluble in this organic reactant medium. It is also known that bulk Keggin structure compounds are thermally not stable beyond 380°C [10].

Peng et al. [11] studied the oxidation of benzyl alcohol over a series of Cs salts of 12-molybdophosphoric acid (MPA) and vanadium incorporated MPA using $H_2O_2$ as oxidant and achieved a maximum conversion of 69.1% with benzaldehyde selectivity of 98.6%. However, the reaction was carried out in the liquid phase batch process.

It was also observed that the decomposition of ammonium cations from the secondary structure and destruction of primary Keggin structure into Mo and P oxides at higher temperatures is responsible for decrease of catalytic performance. Incorporation of transition metals into Keggin structure is one of the known methods to improve the thermal stability of the heteropoly compounds [12]. The metal ions added can either be positioned outside the Keggin unit in the form of cations or directly replace poly atom (Mo or W) in the Keggin anion. The metal ions have considerable effect on the catalytic behavior by influencing the redox properties of the total catalyst or modifying catalyst acid-base properties [13]. Lingaiah et al. [14] used vanadium substituted AMPA as a catalyst and observed increased activity and benzaldehyde selectivity. Authors also observed better enhancement in benzaldehyde selectivity when the vanadium exists as isolated species in the Keggin structured HPA. The same research group also studied the effect of loading of vanadium incorporated AMPA on $TiO_2$ support for the catalytic ammoxidation of 2-methylpyrazine reaction [15]. To best of the knowledge, there is no report available in the literature regarding the addition of Ti to the AMPA and its effect on the structural stability and catalytic performance in selective oxidation of benzyl alcohol.

This report discusses the results on preparation, structural characterization of Ti incorporated AMPA calcined at temperature range of 300-500°C.Vapor-phase benzyl alcohol oxidation was carried out as a model reaction to probe the redox properties of Ti incorporated samples.

## 2. EXPERIMENTAL

### 2.1 Preparation of catalysts

The chemicals used for the synthesis of catalytic materials are analytical grade reagents and used as received without further purification. The procedure adopted for the preparation of Ti incorporated AMPA catalyst is as follows. Ammonium heptamolybdate [$(NH_4)_6Mo_7O_{24}$. $6H_2O$] and diammonium hydrogen orthophosphate $(NH_4)_2HPO_4$ [Loba Chemi, India] were added into minimum amount of water, and completely dissolved at the maximum temperature of 80°C. To this solution a calculated amount of $TiCl_4$, [Loba Chemi, India] in dil. HCl solution is also added. The contents were refluxed at 100°C for 4h, and then required amount of dil. HCl was slowly added to the total solution to maintain the pH of the solution around 2. The addition of acid continued up to the pH of the solution become 1 to obtain a precipitate. The precipitate was filtered and washed with distilled water for four times and dried at 120 °C over night. The dried powder was pretreated at different temperatures of range from 300-500 °C for 4h. The atomic ratio of Mo:Ti has been varied from 11:1, 10:2 and 9:3 for $AMPTi_1$, $AMPTi_2$ and $AMPTi_3$ series of catalysts. For some comparison study, pure AMPA was prepared by acidification of an aqueous solution of ammonium molybdate, phosphoric acid, and the appropriate amount of ammonium nitrate with nitric acid. The resulting suspension was evaporated to dryness and the solid thus obtained was calcined at 300 °C for 4 h.

### 2.2 Characterization of catalysts

The atomic ratios of Mo, Ti, and P were measured by Perkin-Elmer ICPMS. Quantachrome Autosorb was used for the BET surface area determination by nitrogen physisorption at liquid nitrogen temperature (-196°C). The XRD patterns were recorded in a D5000 Seimens X-ray diffractometer using Ni filtered Cu K$\alpha$ radiation ($\lambda$ = 1.5405 Å). FTIR spectra of fresh and used catalysts were recorded on a Bruker D70 spectrometer. Thermograms of the samples were obtained on a Netsz thermal analyzer. Samples about 5 mg in weight were heated to 700 °C in Alumina sample pan under a helium gas flow at a constant heating rate of 10 °C/min. $^{31}P$ MAS NMR spectra of solids were recorded in a 400 MHz Bruker spectrometer. A 4.5 μs pulse (90°) was used with repetition time of 5s between pulses in order to avoid saturation effects. Spinning rate was 10 kHz. All the measurements were carried out at room temperature using $(NH_4)_2HPO_4$ as standard reference. The UV-vis diffuse reflectance spectra of the samples were obtained by a Varian Super Scan 3 UV–vis spectrophotometer fitted with a diffuse reflectance chamber.

The acid strength of the catalysts was measured by using the potentiometric titration method. A known amount of catalyst (about 0.1 g) was suspended in acetonitrile and stirred for about 3 h. Later, the suspension was titrated with a solution of 0.05 N *n* -butyl amine in acetonitrile at a flow rate of 0.5 ml/min using a micro-processor controlled titrater (Schott, Germany). The variation in electrode potential, while adding the *n*-butyl amine solution, was measured using a double junction electrode. In recent times, the potentiometric method has been gaining prominence over the other methods taking into account that the acid and base functionalities of a solid are not properly defined thermodynamically. This method is based on the principle that the acidic environment around the electrode membrane mainly determines the potential difference. The measured electrode potential is an indicator of the acid strength of the dispersed solid.

### *2.3 Catalytic oxidation of benzyl alcohol oxidation*

Vapor phase aerobic oxidation of benzyl alcohol was carried out in a fixed bed micro reactor at atmospheric pressure. In a typical experiment about 1 g of catalyst (crushed to a particle size of 18/25 BSS mesh to avoid mass transfer limitations), diluted with same size and volume of quartz beads, was loaded in a micro reactor. The catalyst was initially pre-treated in air (60 ml/h) at 300 $^{o}$C for 1 h. The reactant, benzyl alcohol, was fed into the reactor at a flow rate of 2 ml/h using a microprocessor based syringe pump (B. Braun, Germany). Pre-heated air was also introduced at a rate of 60 ml/min. The reaction was carried out in the temperature range of 250-310 $^{o}$C. After the system had attained steady state over a period of 1 h, the liquid product collected (by cooling it to approximately 10 $^{o}$C) was analyzed by gas chromatography with SE-30 column and a flame ionization detector.

## 3. RESULTS AND DISCUSSION

The thermal stability of as synthesized samples was investigated by thermogravimetric (TG) analysis. The TG patterns of $AMPTi_1$, $AMPTi_2$ and $AMPTi_3$ showed in Figure 1. Thermolysis of AMPA generally occurs in three steps as described in following three equations. The TG curve shows that there are two steps of weight loss in case of $AMPTi_1$ and $AMPTi_2$ and three steps of weight loss in $AMPTi_3$ case. In both $AMPTi_1$ and $AMPTi_2$, the first step is observed between 140 and 360$^{o}$C and this is due to the loss of crystalline water and loosely bounded ammonia (eqn.1). The second step between 360 and 540$^{o}$C is due to complete loss of ammonia as divalent nitrogen to form anhydrous acid and loss of oxygen atoms to form mixture of oxides [16].

$$(NH_4)_3PMo_{12}O_{40} . 4H_2O \quad \rightarrow \quad (NH_4)_{1.67}H_{1.33}PMo_{12}O_{40} + 1.33NH_3 + 4H_2O \quad (1)$$

$$(NH_4)_{1.67}H_{1.33}PMo_{12}O_{40} \quad \rightarrow \quad H_8PMo_5^{5+} Mo_7^{6+}O_{40} + 0.835N_2 \quad (2)$$

$$H_8PMo_5^{5+}Mo_7^{6+}O_{40} \quad \rightarrow \quad [PMo_5^{5+}Mo_7^{6+}O_{36}] + 4H_2O \quad (3)$$

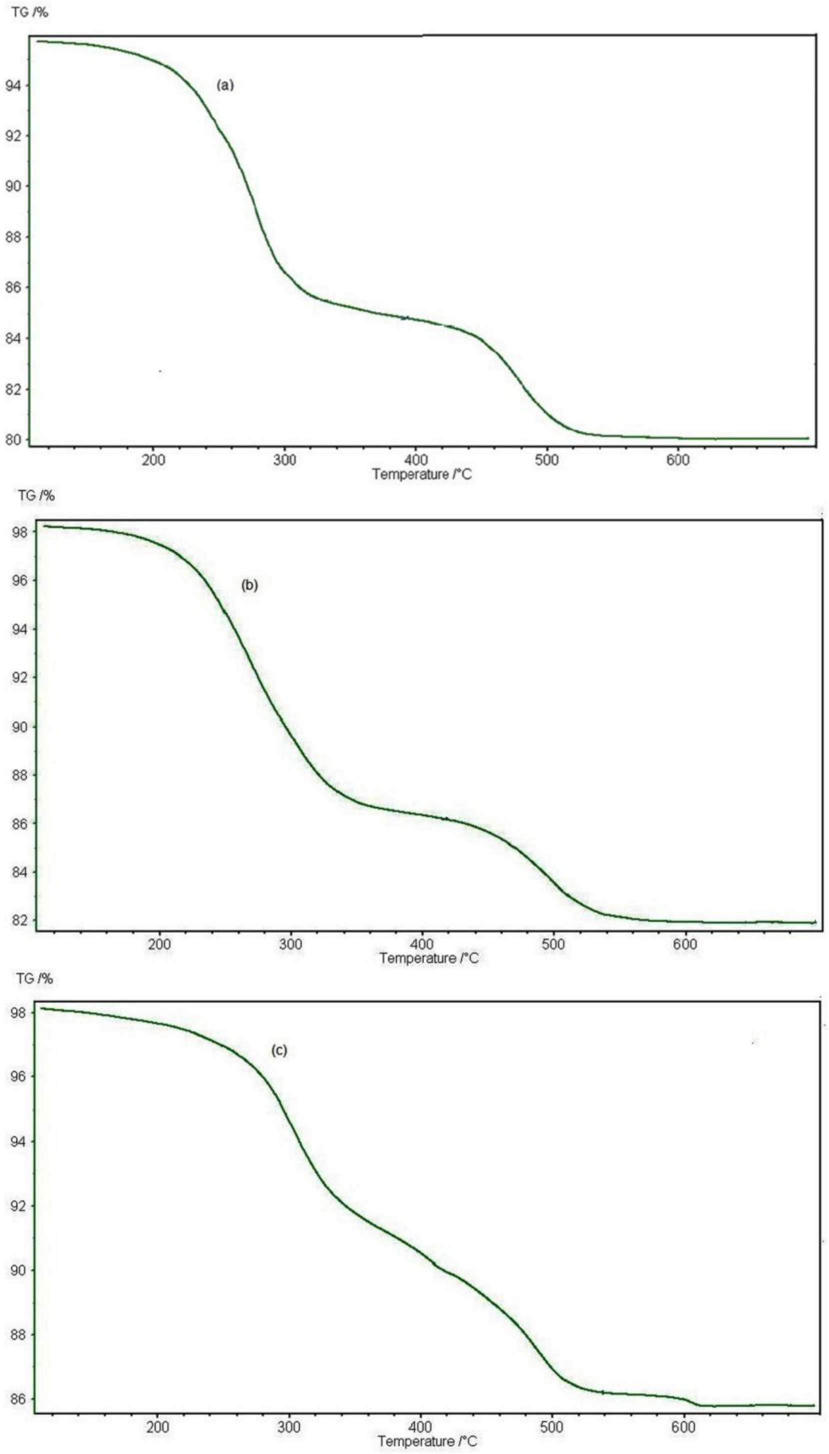

**Figure 1**. TG patterns of as synthesized (a) AMPTi$_1$ (b) AMPTi$_2$ and (c) AMPTi$_3$ samples

The complete destruction of Keggin ion occurs beyond 420$^{o}$C in case pure AMPA sample [16]. This process is clearly delayed in Ti incorporated samples. Most probably the Ti atoms are replacing the ammonium or proton cations in the dehydrated product of thermolysis (eqn. 2 & 3) and stabilizing the Keggin ion. This effect was observed in all Ti incorporated AMPA samples and it was more intense in case of AMPTi$_3$. In AMPTi$_3$ sample, an additional step of weight loss was observed between

540 and 620°C. The total weight loss is of 20, 18 and 14 wt.% for $AMPTi_1$, $AMPTi_2$ and $AMPTi_3$ respectively. It is to note that the amount of weight loss from Ti incorporated samples is higher than that of pure AMPA (around 11 wt.%). The increase of Ti cations in the Keggin structure leads to decrease of existence of protons and ammonium ions in the structure of thermolysis product. It is reported that when the metallic cations are hydrated in the crystal $[M(H_2O)_x]^{n+}$ species, the loss of such molecules of water could be observed at higher temperatures [17]. It was also observed that number of water molecules coordinated to metal ion is depending on the metal nature. Some of them within clusters, such as $H_3O^+$ or $H_5O_2^+$, are more tightly bound in the crystal structure [18]. So, the additional weight loss in Ti incorporated samples could be attributed to the loss of water corresponding to the hydrated Ti cation.

The surface areas of the $AMPTi_1$, $AMPTi_2$ and $AMPTi_3$ catalysts calcined at different temperatures in the range of 300-500°C are tabulated in Table 1.

**Table 1**. Surface area and elemental composition of the samples

| Catalyst | Calcination temperature (°C) | Number of Ti atoms | Surface area ($m^2 g^{-1}$) | Elemental analysis (ICP-MS) | |
|---|---|---|---|---|---|
| | | | | P/Mo atomic ratio | P/Ti atomic ratio |
| AMPA | 300 | 0 | 125.0 | 0.10 | n/a |
| AMPA | 400 | 0 | 85.0 | 0.12 | n/a |
| AMPA | 500 | 0 | 10.0 | 0.15 | n/a |
| $AMPTi_1$ | 300 | 1 | 110.0 | 0.12 | 1.00 |
| $AMPTi_1$ | 400 | 1 | 50.0 | 0.17 | 1.70 |
| $AMPTi_1$ | 500 | 1 | 6.0 | 0.29 | 2.40 |
| $AMPTi_2$ | 300 | 2 | 100.0 | 0.14 | 0.54 |
| $AMPTi_2$ | 400 | 2 | 40.0 | 0.20 | 1.08 |
| $AMPTi_2$ | 500 | 2 | 4.0 | 0.32 | 1.40 |
| $AMPTi_3$ | 300 | 3 | 82.0 | 0.16 | 0.48 |
| $AMPTi_3$ | 400 | 3 | 33.0 | 0.20 | 0.55 |
| $AMPTi_3$ | 500 | 3 | 4.0 | 0.31 | 0.68 |

In general, the dried ammonium salts of heteropolyacids are possessing micro pores. A decrease in the surface area occurred on heating of the AMPA sample from 300 °C to 500 °C (85 to 10 $m^2 g^{-1}$), similar to that reported by other investigators [19]. It is known fact that treatment at high temperature leads to decrease of the ammonium content in the secondary structure of the Keggin HPAs. At very high temperatures (beyond 420 °C), formation of Mo and P oxides results a drastic decrease of surface area of the catalysts. Decrease in surface area with the addition of Ti contributing to high surface coverage implies pore blockage [20].

The amount of Ti incorporated into the heteropoly compound structure was analyzed by ICP-MS and the results are tabulated in Table 1. The P/Ti ratio in all three the series of catalysts calcined at 300 °C are quite matching with theoretical ratio. With increasing the calcination temperature, P/Ti ratios are apparently higher than theoretical ratio. P/Mo ratio decreases markedly with the increase in Ti atomic ratio and it is slightly lower than that added in the solutions during preparation. These results indicate that the stochiometirc P, Mo and Ti ratios were maintained when the crystalline structure of AMPA was intact (below 400 $^oC$). It appears that increase of calcination temperature beyond 400 $^oC$ caused expulsion of certain amount of Ti species out of the HPA structure.

The XRD patterns of fresh AMPTi$_1$, AMPTi$_2$ and AMPTi$_3$ catalysts pretreated at different temperatures in the range of 300-500$^o$C are shown in Figures 2 A, B & C respectively. All the catalysts calcined at 300$^o$C and 350$^o$C possessed stable cubic secondary structure of $(NH_4)_3PMo_{12}O_{40}.4H_2O$ (JCPDS File No.9-412).

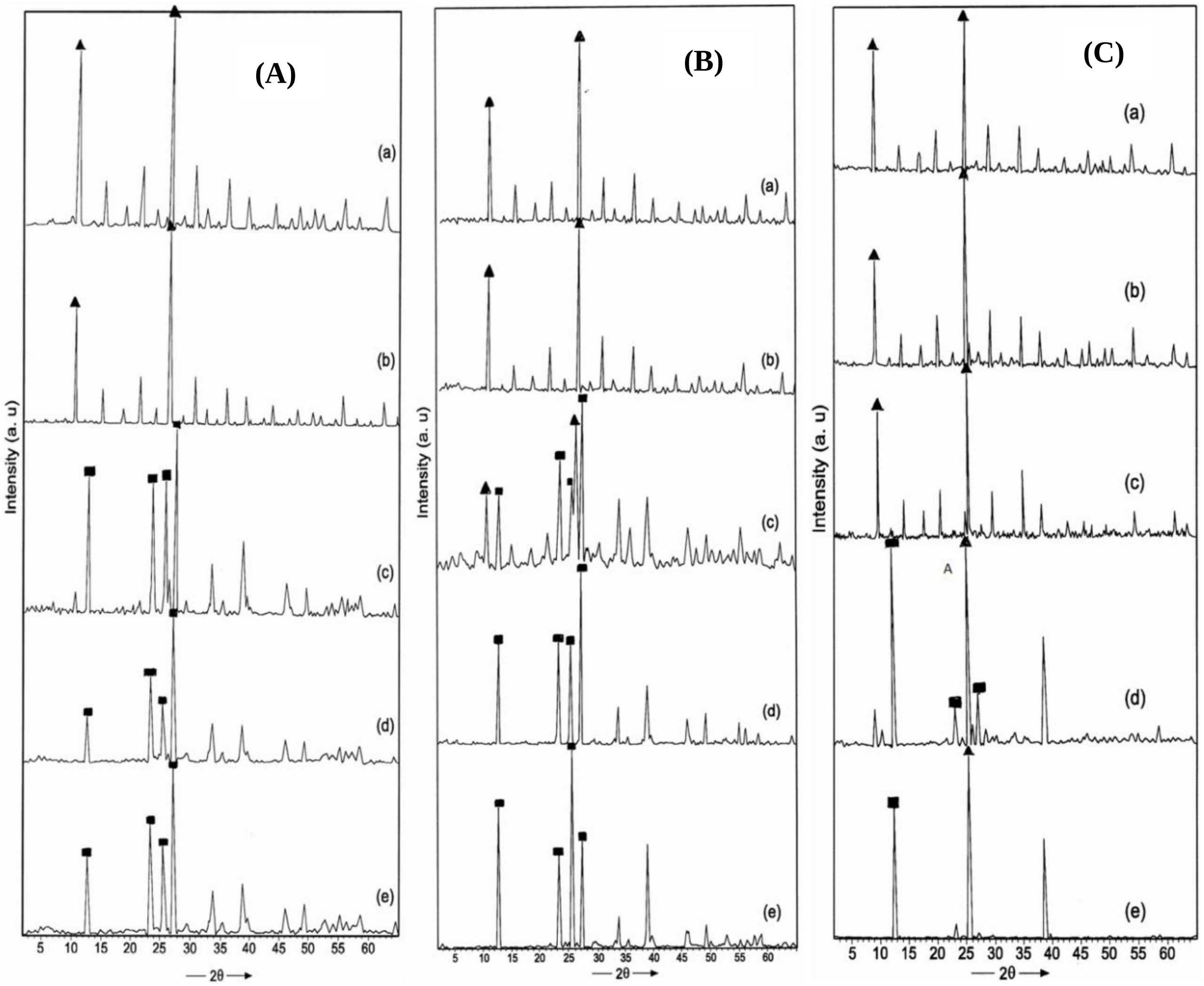

**Figure 2**. XRD patterns of (A) AMPTi$_1$ (B) AMPTi$_2$ (C) AMPTi$_3$ calcined at (a) 300$^o$C, (b) 350$^o$C (c) 400$^o$C (d) 450$^o$C (e) 500$^o$C, ▲= $(NH_4)_3PMo_{12}O_{40}.4H_2O$, ■ = $MoO_3$

Appearance of intensive diffraction peaks corresponding to $\alpha$-$MoO_3$ (Molybdenite, JCPDS 35-0609) is started in the AMPTi$_1$ and AMPTi$_2$ samples pretreated at 400$^o$C along with minor diffraction peaks corresponding to AMPA. This is due to decomposition of ammonium salt has started in the case of $AMPTi_1$ and $AMPTi_2$ at this temperature. It was reported that cubic lattice of pure ammonium salt is maintained until 390°C and at higher temperature than 390°C; the ammonium cations are decomposed with the release of ammonia and constitutional water as observed in the literature report [21]. The sample $AMPTi_3$ calcined at 400°C showed diffraction peaks corresponding to $(NH_4)_3PMo_{12}O_{40}.3H_2O$ (JCPDS No.16-181) and did not showed any diffraction peaks corresponding to $\alpha$-$MoO_3$. At 450°C and 500°C, $AMPTi_1$ and $AMPTi_2$ samples showed major diffraction peaks due to $\alpha$-$MoO_3$ resulting of decomposition of Keggin.

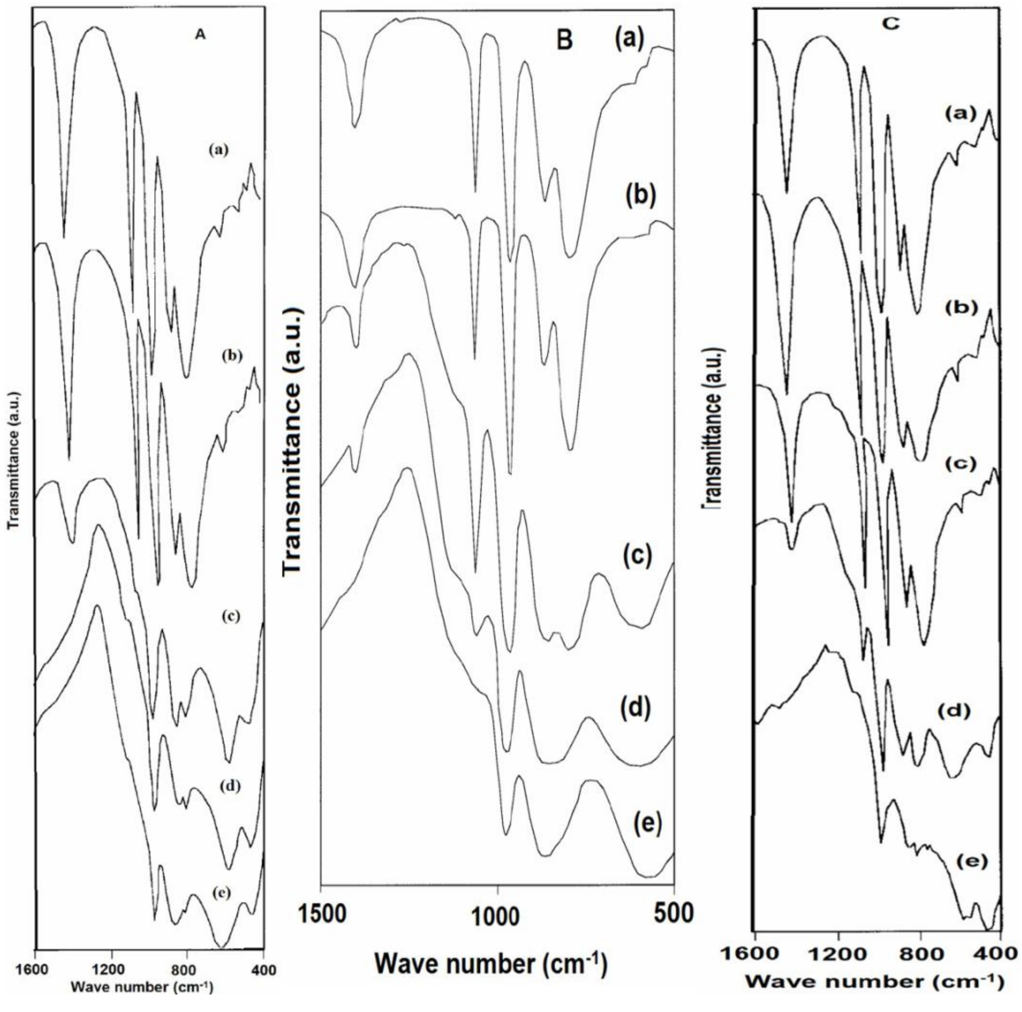

**Figure 3**. FTIR of (A) $AMPTi_1$ (B) $AMPTi_2$ (C) $AMPTi_3$ calcined at (a) 300°C, (b) 350°C (c) 400°C (d) 450°C (e) 500°C

On the other hand $AMPTi_3$ sample showed major diffraction peaks corresponding to AMPA trihydrate at these high temperatures. The XRD data indicating that the addition of Ti has delayed the thermal decomposition of Keggin ions. These results are quite corroborating with the observations from TG results. It has been reported in several publications that, when there is a sufficient quantity of guest metal available in the Keggin structure, the guest metal could replace the Mo in peripheral positions in the Keggin anion or it could also act as cation by replacing the proton or ammonium ions in the secondary structure [22]. Marchal-Roch et al. [23] prepared vanadyl ammonium salt $(NH_4)_{3-}$

$_{2x}(V^{VI}O)_x[PMo_{12}O_{40}]$ by reacting heterogeneous reaction between $H_3[PMo_{12}O_{40}]$ and a toluene solution of the metal acetylacetonate $[VO(acac)_2]$. Same authors also prepared vanadium incorporated in Keggin anion, $(NH_4)_4[PMo_{11}V^VO_{40}]$ by adding ammonium precursor to $H_4[PMo_{11}V^VO_{40}]$. Evaluation of the X-ray pattern of $(NH_4)_4[PMo_{11}V^VO_{40}]$ at different temperatures revealed that the cubic phase is stable up to 410 $^oC$. In case of $(NH_4)_{3-2x}(V^{VI}O)_x[PMo_{12}O_{40}]$ the cubic phase is maintained only until 390 $^oC$. The temperature difference is not a high, however, Sultan et al. [24] proposed that in case of $(NH_4)_4[PMo_{11}V^VO_{40}]$, vanadium atoms can easily removed by a simple thermal treatment at 210 $^oC$ from the Keggin anion and $V^v$cations could take a counter-cation position in place of protons or be expelled from the heteropolyacid structure to form an independent species. There is a possibility that a similar phenomenon could be taking place in case of Ti incorporated AMPA samples.

FTIR analysis is the finger print technique to analyze the structural changes of HPA compounds. The FTIR spectra of the fresh $AMPTi_1$, $AMPTi_2$ and $AMPTi_3$ catalysts pretreated at different temperatures in the range of 300-500$^oC$ are shown in Figure 3 A, B & C respectively. The FTIR spectrum of the AMPA pretreated at 300$^oC$ generally shows the peaks at 1065, 964, 887, 790 and 1420 $cm^{-1}$ corresponding to $\nu_{as}(P\text{-}O_d)$, $\nu_{as}(Mo\text{-}O_t)$, $\nu_{as}(Mo\text{-}O_b\text{-}Mo)$, $\nu_{as}(Mo\text{-}O_c\text{-}Mo)$ and $NH_4^+$ vibrations respectively [16]. All the series of samples calcined at temperature in the range of 300-400$^oC$ showed the presence of all the characteristic peaks of Keggin primary structure as well the peak at 1420$cm^{-1}$ due to the ammonium ion (secondary structure). These results are offering clear evidence that the Keggin primary structure is preserved up to 400 $^oC$ in all Ti incorporated samples. At 450$^oC$, $AMPTi_1$ sample did not show any peak corresponding to $NH_4^+$ ion and peaks due to $MoO_3$ at 982, 863 and 595 $cm^{-1}$ clearly appeared, but at this temperature, $AMPTi_2$ and $AMPTi_3$ samples showed peaks due to Keggin and ammonium ions. At 500$^oC$, $AMPTi_1$ and $AMPTi_2$ samples showed peaks only due to $MoO_3$, but the $AMPTi_3$ sample showed the small peaks due to Keggin ion and the peak due to ammonium ion was disappeared. These results are clearly indicating that the Keggin primary structure is stable below 450$^oC$ for $AMPTi_1$, below 500$^oC$ for $AMPTi_2$ and stable above 500$^oC$ for $AMPTi_3$ sample. With increase of Ti content, increase of thermal stability of Keggin structure was observed from FTIR spectral data.

The questions need to answer at this juncture are, where the Ti atoms are situated? And how Ti atoms are stabilizing the Keggin ion at high temperatures? If any transition metal is substituted in place of Mo in the Keggin anion, the metal induces alterations in the IR spectrum that allow monitoring the presence of the metal inside the Keggin structure [18]. The previous works revealed that substituting metal induces a decrease of the oxoanion symmetry, leading to a split of the asymmetric (P-O) stretching band. As a consequence, a shoulder should be observed in the (P-O) band of the Ti incorporated samples. The FTIR spectral data of Ti incorporated samples showed no differences in the structure due to the Ti addition with respect to the pure AMPA. From these results, it is easy to understand that Ti did not replace the Mo in peripheral positions in Keggin anion. These results are indicating that added Ti atoms are acting as cations in secondary structure or forming an amorphous segregated oxide phase.

Albonetti et al. [25] observed some changes in FTIR spectrum, when a Mo atom in the Keggin anion was substituted by a vanadium (V) atom. More particularly a splitting of the asymmetric P-O stretching band appeared and consequently a shoulder was observed at 1060 $cm^{-1}$ that was not present in the P-O band of the parent acid, MPA. Upon calcination of V substituted HPA at 300°C, the shoulder was completely disappeared suggesting that the V atoms were largely expelled from the Keggin primary units. Knapp et al. [20] also concluded same point by combining the TG and FTIR results of Fe incorporated AMPA samples. When the samples contained Fe atom in the Keggin primary anion, the temperature of $NH_3$ removal was shifted down to 200°C, from 390°C of the AMPA and a shoulder at P-O stretching vibration was disappeared for the sample treated at 200°C. The release of Fe from the Keggin anion at low temperature can thus be attributed to the reaction of $Fe^{3+}$ with the $NH_4^+$ counter-ion, which is oxidized to ammonia or nitrogen, and eliminated from the secondary structure. The authors also discussed two possible reasons for this to happen. First one, the oxidation of $NH_4^+$ leads to a $Fe^{2+}$ product, which might compromise the stability of the Keggin unit and might therefore be released. Second one, the $NH_3$ elimination is an exothermic reaction that might lead to hot spots that would drive to the Fe release from the Keggin unit. In the present study, it appears that the Ti atoms were inside of the Keggin primary structure as an amorphous oxide phase before the thermal treatment. During the thermal treatment the Ti ions were expelled out of primary Keggin ion and acted as cations in the secondary structure as we can observe the presence of Keggin structure in the Ti incorporated samples up to 400 °C (XRD results).

The structural aspects of the catalysts were further investigated by $^{31}P$ MAS NMR technique because $^{31}P$ MAS NMR technique is very sensitive to local chemical environment and surrounding symmetry of phosphorous. Solid state $^{31}P$ MAS NMR spectra of Ti incorporated AMPA catalysts before calcination is shown in Fig. 4. The MAS NMR study was performed at room temperature without degassing the samples. $AMPTi_1$ sample showed total four peaks, a major sharp peak at -4.6ppm, a small sharp peak at -5.8ppm, a broad peak centered at-1.3 ppm and another small broad peak at 7.7ppm. All the samples displayed more than one phosphorus resonance, clearly indicating that the structure of heteropolyacid salts is complex. According to Black et al [26], pure $(NH_4)_3PMo_{12}O_{40}.4H_2O$ reflects a single chemical shift at -4.45 ppm. The peak appeared at -4.6 ppm can be assigned to pure AMPA. It is known that the $^{31}P$ MAS NMR chemical shift is strongly dependent on the number of water molecules presented in its structure, for instance, chemical shift of $^{31}P$ has been found at -3.9 ppm for $H_3PMo_{12}O_{40}\cdot 30H_2O$, -2.9 ppm for $H_3PMo_{12}O_{40}$ [27]. It is also reported that metal substitution in Keggin ion can lead to mixtures containing a variety of species with differing degrees of substitution. A small peak occurred near the main peak, with $\delta$ = -5.8 ppm, probably due to the portions of the sample having different degrees of hydration. van Veen et al. [28] reported the appearance of peak at -1.5 ppm for the sample dried at room temperature and they assigned this peak to lacunary $[PMo_{11}O_{39}]^{7-}$ phase. The broad peak at 7.7 ppm could be due to unreacted phosphate presented in the as synthesized sample. $AMPTi_2$ and $AMPTi_3$ samples showed same four peaks, but the intensity of three peaks at -5.8, -1.3 and 7.7 ppm decreased. It is very interesting to note that the peak at 7.7ppm, which is assigned to unreacted phosphate, is almost disappeared in case of $AMPTi_3$ sample. This could be due to availability of extra Ti atoms to react with the lacunary and phosphate ions.

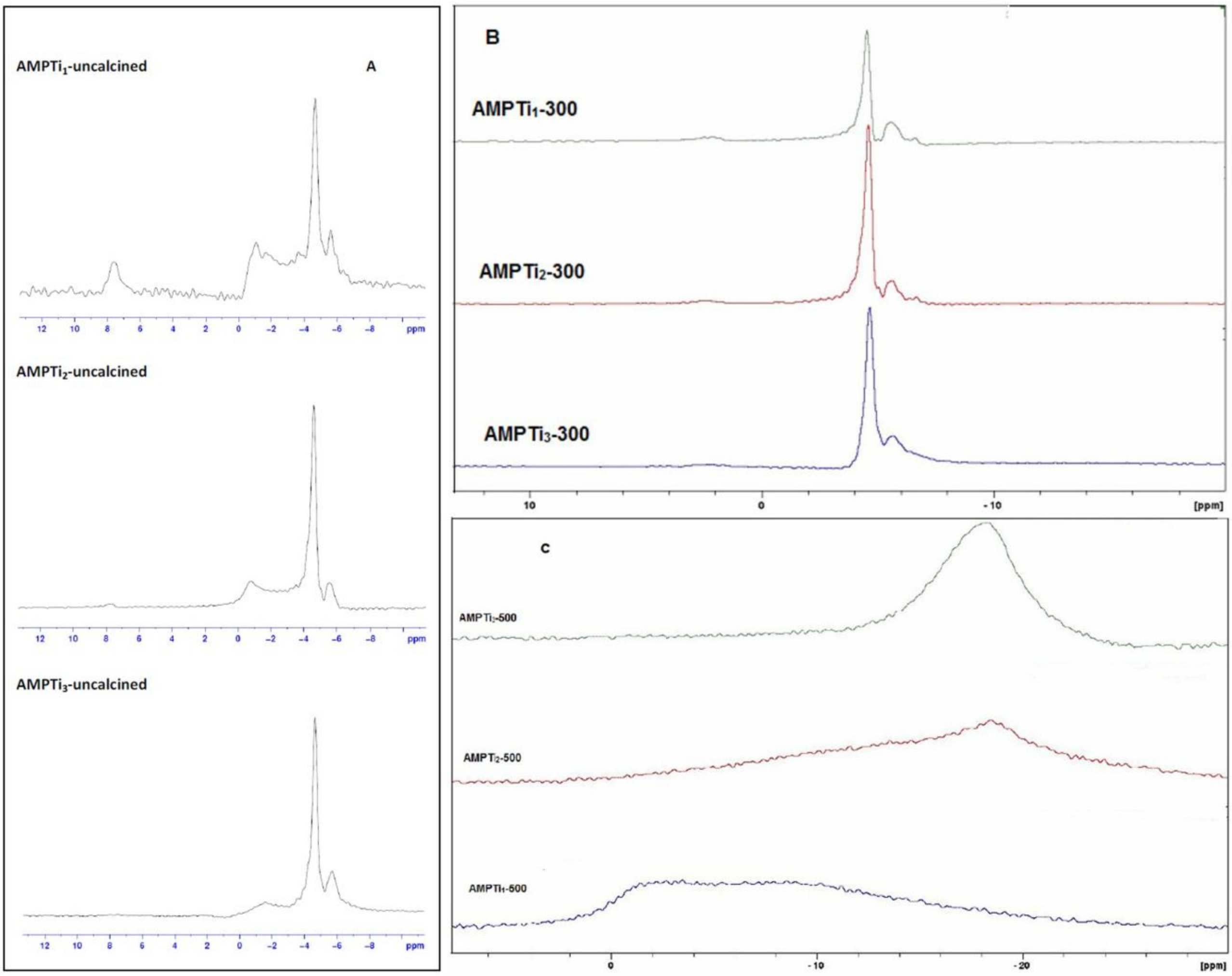

**Figure 4**. $^{31}$P MAS NMR spectra of uncalcined and calcined Ti incorporated AMPA catalysts

After treatment at 300°C, AMPTi$_1$ showed an intense sharp peak at -4.6 ppm and small broad peak at -5.8 ppm. With increase of Ti atoms from 2 to 3 in AMPA, the intensity of small broad peak increases and another small peak started appearing at -6.5 ppm. The new peak at -6.5 ppm probably due to some lattice distortion associated to the inclusion of the guest Ti atoms. Damyanova et al. [29] explained how the presence of transition metal in silica based support would influence the chemical shift values ($\delta$) of MPA. They observed a new peak at -7 ppm apart from the bulk and dehydrated MPA and they assigned that peak to species that would be caused by a strong interaction of MPA with the Zr cation. We could assign the new peak at -6.5 ppm to the Ti and AMPA interactive species.

After heating the materials up to 400°C, AMPTi$_1$ sample showed a major peak at 0 ppm, a small broad peak at -8.2 ppm and a broad hump centered at -4.5 ppm. The peak at 0 ppm is due to the phosphorous oxides formed due to decomposition of Keggin ion and the peak at -8.2 ppm could be attributed to the lacunary species. AMPTi$_2$ sample also exhibits three peaks, a major peak at 0ppm, a small hump at -1.9 ppm and a small peak at -4.5 ppm. On other hand, AMPTi$_3$ sample showed a major sharp peak at -4.0 ppm with a small tail at -4.5 ppm and two other peaks at 0 ppm and -8.2 ppm respectively. These results are clearly indicating that a prominent decomposition was occurred in

AMPTi$_1$ sample at 400 $^o$C and the same process is also existed in AMPTi$_2$ and AMPTi$_3$ samples, but the extent of decomposition is less in case of AMPTi$_3$ than the rest of the two samples. It is interesting to observe a well organized Keggin ion decomposition pattern from these spectra and also to see the stabilization effect of Ti atoms.

All the samples calcined at 500$^o$C showed broad peaks composed of at least three peaks. AMPTi$_1$ showed a big envelope started from 0 ppm to -20 ppm and AMPTi$_2$ and AMPTi$_3$ yielded broad peak centered at -19.4 ppm. According to Iwamoto et al. [30] these peaks can be assigned for mono and polyphosphates formed during the calcination. The spectrum of AMPTi$_3$ is relatively more uniform than AMPTi$_2$ and AMPTi$_3$ samples. The multiple bands represented by the AMPTi$_1$ and AMPTi$_2$ samples indicate the uneven decomposition of Keggin unit into different polymeric phosphorus oxo species. In contrast, AMPTi$_3$ sample showed presence of single polymeric species suggesting the positive effect of incorporation of more Ti atoms in HPA structure. Bhumik reported that tetrahedral phosphorous in microporous aluminophosphate materials shows a strong band at around -28 ppm [31]. $^{31}$P MAS NMR spectra of the titanium phosphate samples showed a broad signal with chemical shifts between 10 to -25 ppm [32]. The observed chemical shift at -19.4 ppm and peak shape of the AMPSb$_3$ sample calcined at 500 $^o$C is very close agreement and this peak could be assigned to titanium phosphate structure.

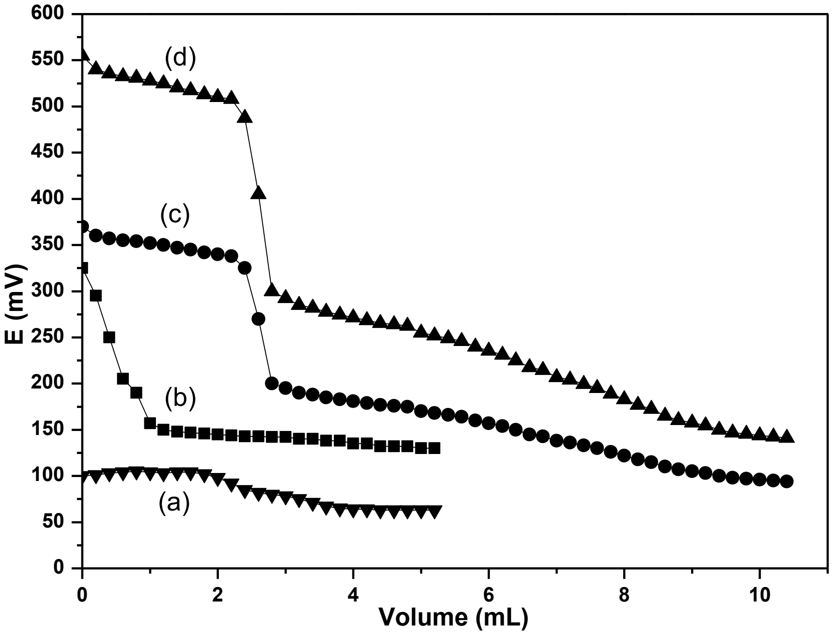

**Figure 5.** Potentiometric titration curves for (a) AMPA (b) AMPTi$_1$ (c) AMPTi$_2$ (d) AMPTi$_3$ catalysts calcined at 300 $^o$C

The potentiometric titration curves obtained for the catalysts during the *n*-butyl amine titration are shown in Fig. 5. Pizzio et al. [33] applied this technique to evaluate the strength and the total number of acid sites on HPA catalysts. In order to interpret the results it is suggested that the initial electrode potential (Ei) be taken as the acid strength of the surface sites and the range, where the plateau is reached as the total number of acid sites. The acid strength of surface sites can be assigned according to the following ranges: very strong site, $E_i > 100$ mV; strong site, $0 < E_i < 100$ mV; weak site, $-100 < E_i < 0$ mV, and very weak site, $E_i < -100$ mV [34]. In the present study the acidic strengths of AMPA and Ti incorporated AMPA catalysts are found to be very strong (Fig.6). The Ti incorporated catalysts showed high measured electrode potential implying the presence of stronger acid sites than AMPA catalyst.

When the metallic cations are hydrated in the crystal $[M(H_2O)_x]^{n+}$ species causes the change in the charges on the different oxygen atoms of Keggin primary structure, mainly bridging oxygen, leading to higher acid strength of a new proton [35]. With increase of Ti content increase in the acidity was observed. As reported previously, acidic properties of HPA compounds are sensitive to counter cations constituent elements of polyanions, and tertiary structure. Partial hydrolysis and in homogeneity of composition brought about during preparation are also important in governing the acidic properties; there are at least two possible types of origins of acidity of Ti incorporated AMPA catalysts.

1. Dissociation of coordinated water;

$$[Ti(H_2O)_m]^{n+} \rightarrow [Ti(H_2O)_{m-1}(OH)]^{(n-1)} + H^+$$

2. Lewis acidity of metal ions

With the present information on surface acidity it is not possible to assess the type of acid sites (Bronsted or Lewis) existing on the surface of the catalysts, as the potentiometric titration cannot distinguish between the two. However, these data help to compare the performance of the catalysts.

UV-Visible diffuse reflectance technique was used to probe how the electronic properties of the Mo ions were affected by the presence of Ti ions. In the UV-Vis spectra of AMPA, $AMPTi_1$, $AMPTi_2$ and $AMPTi_3$ samples calcined at 300 °C are shown in Fig. 6. A wide band in the domain of wavelengths 200-400 nm was observed for all the samples. It was reported that ligand-metal charge transfers (LMCT) from oxygen to Mo(VI) in the Keggin anion is responsible for the broad band [36].

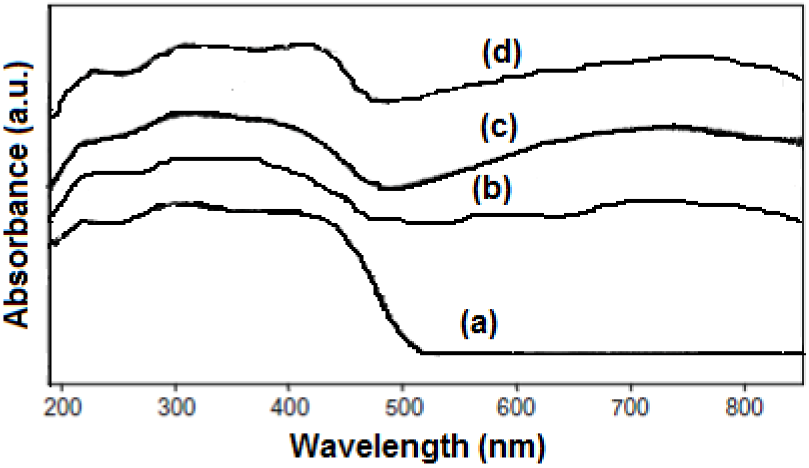

**Figure 6.** UV-Vis spectra for (a) AMPA (b) $AMPTi_1$ (c) $AMPTi_2$ (d) $AMPTi_3$ catalysts calcined at 300 °C

The literature reports are suggesting that the appearance of several bands in the UV-Vis spectrum of Keggin-type HPA could be due to different oxygen ions and to inter-anion charge transfer transitions [37]. An additional large charge transfer band above 700 nm for all Ti incorporated samples, which could be attributed to the d-d transition band of Mo(V) species in octahedral coordination [38]. This result suggested a partial reduction of Mo(VI) to Mo(V) in these samples corresponding to the electron exchange occurring between Ti(IV) and Mo(VI) as shown in eqn. (4).

$$Ti^{IV} + Mo^{VI} \leftrightarrow Ti^{V} + Mo^{V} \quad (4)$$

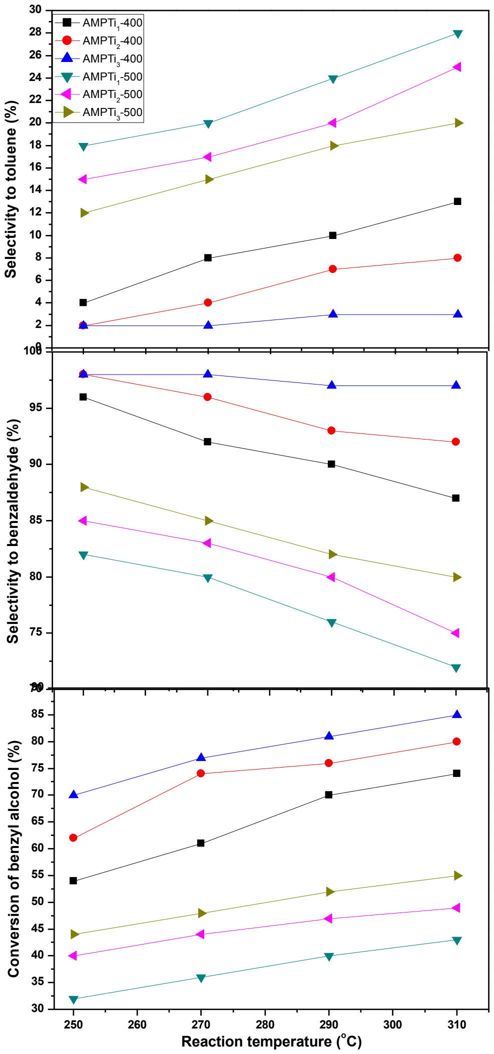

**Figure 7**. Benzyl alcohol oxidation activity over Ti incorporated AMPA catalysts at different reaction temperatures

It is interesting to observe that intensity of this band was increased with increase of Ti atoms. This observation is a direct consequence of increase of concentration of Mo(V) ions with increase of Ti atoms in HPA structure. Thus, UV-Vis spectroscopy results suggest that the extent of reduction of Mo(VI) is higher in case of AMPTi$_3$ sample than AMPTi$_2$ and AMPTi$_1$.

Benzyl alcohol undergoes different transformations based on the nature of the catalyst. The main reactions are:

$$2C_6H_5CH_2OH + O_2 \rightarrow 2C_6H_5CHO + 2H_2O \tag{5}$$

$$2C_6H_5CH_2OH \rightarrow C_6H_5CH_2OCH_2C_6H_5 + H_2O \tag{6}$$

$$2C_6H_5CH_2OH \rightarrow C_6H_5CHO + C_6H_5CH_3 + H_2O \tag{7}$$

The main products observed during the partial oxidation of benzyl alcohol were benzaldehyde and toluene. The benzyl alcohol conversion and selectivities to benzaldehyde and toluene, as a function of reaction temperature, over Ti incorporated AMPA catalysts calcined at 400$^o$C and 500 $^o$C, are shown in Fig. 7.

AMPTi$_1$ calcined at 400 $^o$C offered 54% conversion with 96% selectivity to benzaldehyde at 250$^o$C. AMPTi$_2$ and AMPTi$_3$ catalysts showed 62% and 70% conversion with 98% benzaldehyde selectivity at the same reaction temperature. Increase of Ti content in AMPA structure increased the benzyl alcohol conversion and benzaldehyde selectivity. Similar behavior was observed in other reaction temperatures. With increase of reaction temperature increase in conversion and decrease in selectivity to benzaldehyde was observed. With increase of calcination temperature from 300 to 500$^o$C, all the samples showed an increase in conversion and decrease in selectivity to benzaldehyde.

**Table 2**. Comparison of benzyl alcohol oxidation activity of AMPA and Ti incorporated AMPA catalysts

| Catalyst | AMPA-300 | | | | AMPTi$_1$-300 | | | | AMPTi$_2$-300 | | | | AMPTi$_3$-300 | | | |
|---|---|---|---|---|---|---|---|---|---|---|---|---|---|---|---|---|
| Reaction temperature ($^o$C) | 250 | 270 | 290 | 310 | 250 | 270 | 290 | 310 | 250 | 270 | 290 | 310 | 250 | 270 | 290 | 310 |
| Conversion of benzyl alcohol (%) | 41 | 55 | 57 | 50 | 52 | 60 | 68 | 72 | 61 | 72 | 75 | 78 | 70 | 76 | 81 | 83 |
| Selectivity to benzaldehyde (%) | 93 | 83 | 82 | 75 | 95 | 90 | 87 | 85 | 96 | 92 | 90 | 89 | 98 | 96 | 94 | 94 |
| Selectivity to toluene (%) | 7 | 17 | 18 | 25 | 5 | 10 | 13 | 15 | 4 | 8 | 10 | 11 | 2 | 4 | 4 | 6 |

The product distribution of oxidation of benzyl alcohol at different reaction temperatures over Ti incorporated AMPA catalysts calcined at 300$^o$C was tabulated in Table 2. With the substitution of Ti into AMPA a considerable increase in the conversion and selectivity towards benzaldehyde were observed compared to the product distribution obtained using AMPA itself. This is a significant observation. By incorporation of more Ti into AMPA (AMPTi$_2$ and AMPTi$_3$) an increase in conversion, than that of $AMPTi_1$, was observed at all the reaction temperatures. However, $AMPTi_1$ catalyst was found to be more selective towards benzaldehyde in comparison with AMPA.

The activity data presented in Fig. 7 and Table 2 suggest that both oxidation and acid catalyzed disproportionation of benzyl alcohol occur on AMPA and Ti incorporated AMPA catalysts. The high activity and selectivity in the case of $AMPTi_3$ catalysts calcined at low temperature might be the manifestation of increased acidity and the redox nature of the catalyst. It is interesting to observe, at this juncture, as to which one predominates. The ratio of benzaldehyde to toluene is a measure of oxidizing power to acidity [9, 14]. The benzaldehyde to toluene ratios observed on AMPA and $AMPTi_3$ catalysts, at a reaction temperature of 310 $^oC$, calculated for the sake of comparison, are 3 and 15.6, respectively. These numbers suggest higher oxidizing ability when Ti is substituted in AMPA catalysts.

It was observed that due to the redox reaction between $[PMo_{12}O_{40}]^{3-}$ and residual $Ti^{4+}$ ions, the oxidation state of Mo was reduced from 6 to 5. This extent of reduction is directly proportional to the Ti content and $AMPTi_3$ sample is consisting of more $Mo^{5+}$ species (UV-Vis data). Presence of reduced molybdenum species ($Mo^{5+}$), which are known to be more active in redox type reactions, is the reason for getting high conversion of benzyl alcohol and selectivity of benzaldehyde over $AMPTi_3$ catalysts.

From obtained catalytic activity results over Ti incorporated AMPA samples, it is clear that oxidation and disproportionation reactions are taking place simultaneous leading to benzaldehyde and toluene. The formation of toluene, as a result of disproportionation predominates on strong acid sites, whereas the formation of benzaldehyde, as product of oxidation of benzyl alcohol is taking place on redox sites. Thus, both acidity and redox properties are competing leading to toluene and oxygenated product (benzaldehyde) respectively.

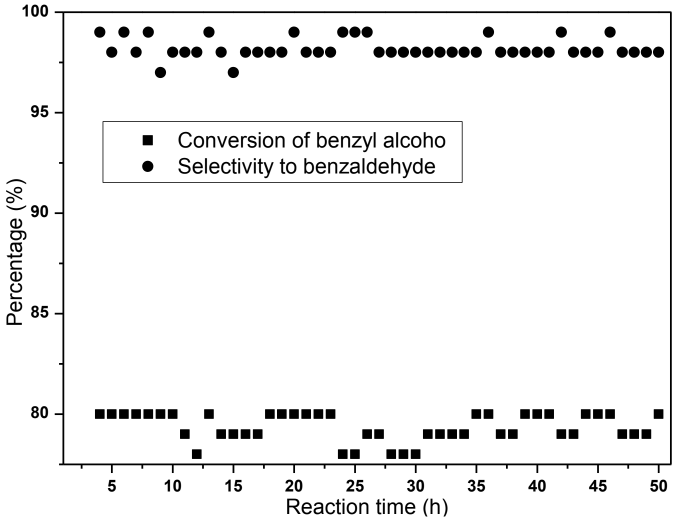

**Figure 8**. Time on stream analysis of $AMPTi_3$ calcined 400 $^oC$

To find out the durability of the catalyst, a time on stream analysis has been carried out on one of the representative catalysts ($AMPTi_3$ calcined at $400^oC$, reaction temperature 310 $^oC$) from the activity pattern shown in Fig.8. It is noteworthy to mention that the catalyst is stable for a period of 50 hours with the conversion of benzyl alcohol between 78-80% and selectivity to benzaldehyde is around 98%. Thus, it is reasonable to conclude that Ti incorporated AMPA catalyst is a better stable redox catalyst for benzyl alcohol oxidation reaction.

## 4. CONCLUSIONS

The AMPA catalysts with amounts of Ti atoms from 1 to 3 and a consequence decrease of Mo atoms from 11 to 9 were synthesized. The new materials were characterized by different characterization techniques. The characterization of catalysts suggests that the Keggin structure was presented in the synthesized catalysts, however Ti atoms do not substitute into the primary structure, but they occupy the cation positions. Incorporation of Ti atoms delayed the thermal decomposition of Keggin structure. The synthesized Ti incorporated AMPA catalysts have stronger acid sites than AMPA. The redox behaviour was determined using oxidation of benzyl alcohol as probe reaction. The extent of $Mo^{6+}$ reduction is directly proportional to the Ti content and $AMPTi_3$ sample is consisting of more $Mo^{5+}$ species (UV-Vis data). Presence of reduced molybdenum species ($Mo^{5+}$), which are known to be more active in redox type reactions, is the reason for getting high conversion of benzyl alcohol and selectivity of benzaldehyde over $AMPTi_3$ catalysts.

ACKNOWLEDGEMENTS
The author thanks Prof. Sulaiman Basahel and Dr. Maqsood Malik for their support.

## References

1. I.K. Song, M.S. Kaba, M.A. Barteau, W.Y. Lee, *Catal. Today* 44 (1998) 285
2. I.K. Song, M.S. Kaba, K. Nomiya, R.G. Finke, M.A. Barteau, *J. Mol. Catal. A* 262 (2007) 216
3. J.J. Altenau, M.T. Pope, R.A. Prados, H. So, *Inorg. Chem.* 14 (1975) 417
4. V.A. Grigoriev, C.L. Hill, I.A. Weinstock, *J. Am. Chem. Soc.* 122 (2000) 3544
5. M. Sadakane, E. Steckhan, *Chem. Rev.* 98 (1998) 219
6. D. R. Park , J. H. Song , S. H. Lee , S. H. Song , H. Kim , J. C. Jung , I. K. Song, *Appl. Catal. A: Gen.* 349 (2008) 222
7. *Ulmann_s Encyclopedia of Industrial chemistry*, fifth ed., vol. A3,VCH Publishers, Weinheim, 1985, p. 469
8. C. Zondervan, R. Hage, B.B. Feringa, *Chem. Commun.* (1997) 419.
9. A. Athilakshmi, B. Viswanathan, in: N.M. Gupta, D.K. Chakraborthy (Eds.), *Catalysis: Modern Trends*, Narosa Publishing House, New Delhi, 1996, p. 311.
10. K-Y. Lee and M. Misono, *Hand Book of Heterogeneous Catalysis*, Eds G. Ertl, H. Knozinger, and J. Weitkamp. Vol.1, p.118
11. Ge Peng, Yonghui Wang, Changwen Hu, Enbo Wang, Shouhuna Feng, Yongchun Zhou, Hong Ding, Yanyong Liu, *Appl. Catal. A*: *Gen.* 218 (2001) 91.
12. M. Misono, and N. Nojiri, *Appl. Catal.A: Gen.*, 64 (1990) 1
13. G. Centi and S. Perathoner, *Catal. Rev.& Sci. Eng.*, 40 (1998) 175

14. N. Lingaiah, K. Mohan Reddy, N. Seshu Babu, K. Narasimha Rao, I. Suryanarayana, P.S. Sai Prasad, *Catal. Commun.* 7 (2006) 245
15. K. Mohan Reddy, N. Lingaiah, K. Narasimharao, Nilofer Rahman, P.S. Sai Prasad, I. Suryanarayana, *Appl. Catal. A: Gen.* 296 (1) (2005) 108
16. C. Marchal-Roch, N. Laronze, R. Villanneau, N. Guillou, A. Teze, and G. Herve, *J. Catal.*, 190 (2000) 173
17. G.A. Tsignidos, *Ind. Eng. Chem. Prod. Res. Dev.* 13 (1974) 267
18. C. Rocchiccioli-Deltcheff, A. Aouissi, M.M. Bettahar, S. Launay, M. Fournier, *J. Catal.* 164 (1996) 16
19. D. Lapham and J. B. Moffat, *Langmuir*, 7 (1991) 2273
20. C. Knapp, T. Ui, K. Nagai, and N. Mizuno, *Catal. Today*, 71 (2001) 111.
21. S. Fujibayashi, K. Nakayama, M. Hamamaoto, S. Sakaguchi, Y. Nishiyama, and Y. Ishii, *J. Mol. Catal. A: Chem.*, 110 (1996) 105.
22. V.M. Bondareva, T.V. Andrashkevich, L. G. Detusheva, and G.S. Litvak, *Catal. Lett.*, 42 (1996) 113
23. C. Marcha-Roch, N. Laronze, N. Guillou, A. Teze, and G. Herve, *Appl. Catal. A: Gen.* 199 (2000) 33
24. M. Sultan, S. Paul, M. Fournier, D. Vanhove, *Appl. Catal. A: Gen.* 259 (2004) 141
25. S. Albonetti, F. Cavani, F. Trifiro, M. Koutrev, *Catal. Lett.*, 30 (1995) 253
26. J. B. Black, and N. J. Clayden, *J. Chem. Soc., Dalton Trans.*, (1984) 2765.
27. A. Bielanski, A. Malecka and L. Kubelkova, *J.Chem. Soc., Faraday Trans.*, 85(9) (1989) 2847
28. J.A.R. van Veen, O. Sudmeijer, C.A. Emeis and H. de Wit, J. Chem. Soc. Dalton Trans. (1986) 1825
29. S. Damyanova Fierro, J. L. G. Sobrados, J. Sanz, *Langmuir*, 15 (1999) 469.
30. R. Iwamoto, C. Fernandez, J. P. Amoureux, and J. Grimblot, *J. Phys. Chem. B*, 102 (22) (1998) 4343
31. A. Bhumik, *Proc. Indian Acad. Sci.* (*Chem. Sci.*), 114 (4) (2002) 451
32. H. Nakayama, T. Eguchi, N. Nakamura, S. Yamaguchi, M. Danjyo and M. Tsuhako, *J. Mater. Chem.*, 7 (1997) 1063
33. L.R. Pizzio, P.G. Vazquez, C.V. Caceres, M.N. Blanco, *Appl. Catal. A: Gen.* 256 (2003) 125
34. P. Villabrille, G. Romanelli, P. Vazquez, C. Caceres, *Appl. Catal. A: Gen.* 270 (2004) 101
35. I.V. Kozhevnikov, K.I. Matveev, *Appl. Catal.* 5 (1983) 135
36. Ch. Srilakshmi, N. Lingaiah, I. Suryanarayana, P.S. Sai Prasad, K. Ramesh, B.G. Anderson, J.W. Niemantsverdriet, *Appl. Catal. A: Gen.* 296 (2005) 54.
37. F. Cavani, R. Mezzogori, A. Pigamo, F. Trifiro, *Chem. Eng. J.* 82 (2001) 33.
38. C. Thomazeau, V. Martin, P. Afanasiev, *Appl. Catal. A: Gen.* 199 (2000) 61.